Supporting Information

NH_3 Plasma Functionalization of UiO-66-NH_2 for Highly Enhanced Selective Fluorescence Detection of U(VI) in Water

Jiali Liu[a], Xianbiao Wang[a]*, Yangyang Zhao[a], Yongfei Xu[a], Yang Pan[b], Shaojie Feng[a], Jin Liu[a], Xianhuai Huang[c], and Huanting Wang[d]

[a] Anhui Province International Research Center on Advanced Building Materials, School of Materials Science and Chemical Engineering, Anhui Jianzhu University, Hefei 230601, PR China

[b] National Synchrotron Radiation Laboratory, University of Science and Technology of China, Hefei 230029, PR China

[c] Anhui Provincial Key Laboratory of Environmental Pollution Control and Resource Reuse, Anhui Jianzhu University, Hefei 230601, PR China

[d] Department of Chemical Engineering, Monash University, VIC 3800, Australia

Corresponding author.

*E-mail address: xbwang@ahjzu.edu.cn (X. Wang).

Table of Contents

Experimental Section

Materials. Ultrapure water was obtained from Adventure-15S water purification equipment. Zirconium chloride ($ZrCl_4$, 98%), 2-aminoterephthalic acid (NH_2-bdc, 98%), glacial acetic acid and DMF were used to synthesize UiO-66-NH_2. All testing nitrates of metal ions (M = UO_2^{2+}, Na^+, K^+, Ag^+, Cu^{2+}, Zn^{2+}, Mg^{2+}, Cd^{2+}, Pb^{2+}, Al^{3+}, Fe^{3+}, Co^{2+}, Ni^{2+}, Ce^{3+}, 4.4×10^{-4} M) were prepared by dissolving in an appropriate amount of ultrapure water.

Instrumentation. The morphology of samples was taken by using a FEI Sirion scanning electron microscope (SEM) and a JEM-2010 high resolution transmission electron microscope (TEM). ATR-FTIR spectra were collected on a Nicolet 6700 spectrometer. The nitrogen adsorption-desorption measurements were performed on a JW-BK122W instrument at 77K, pore size distribution curves were calculated using DFT method. The samples were degassed at 110℃ overnight before measurement. Powder X-ray diffraction data was recorded on a Rigaku diffractometer with scan range of 5-50°. The X-Ray photoelectron spectroscopy (XPS) analysis was performed on a Thermo ESCALAB 250Xi with Al Kα (hv =1486.6 eV) source and the energy analyzer with a fixed transmission energy of 30 eV. The fluorescence spectra of the samples were recorded on a F-4700 (Hitachi) instrument with a width of excitation and emission slit of 5 nm and PMT voltage of 700 V. The UV-Vis diffuse reflectance spectra were performed on a SoildSpec-3700 UV-Vis Spectrophotometer. N content was measured using organic element analysis on an element analyzer (Elementar Unicube, Germany). The fluorescence lifetime was measured with a JY Fluorolog-3-Tou fluorescence spectrophotometer (Jobin Yvon, France). The average results were obtained from 2 valence fitting operation.

UiO-66-NH_2 Preparation. Typically, 0.277 g of $ZrCl_4$ (1.19 mmol) and 0.215 g of 2-aminoterephthalic acid (1.19 mmol) were dissolved in 137 mL of DMF (1.78 mol) and 17 mL of glacial acetic acid (296.70 mmol), and the mixture was sonicated for 20 minutes until fully dissolved. The resulting solution was placed in a 200 mL polytetrafluoroethylene reactor and

the temperature was maintained at 120 ºC for 24 h. After cooling to room temperature, the obtained precipitate was separated by centrifugation and washed sevaral times with DMF and ethanol. Finally, the powder was dried at 100 ºC for 10 h and subsequent activation at 150 ºC for 3 h.

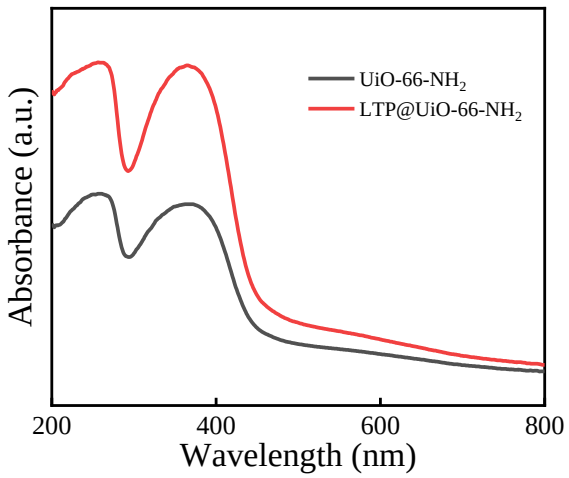

Figure S1. UV-Vis diffuse reflectance spectra of LTP@UiO-66-NH_2 and UiO-66-NH_2.

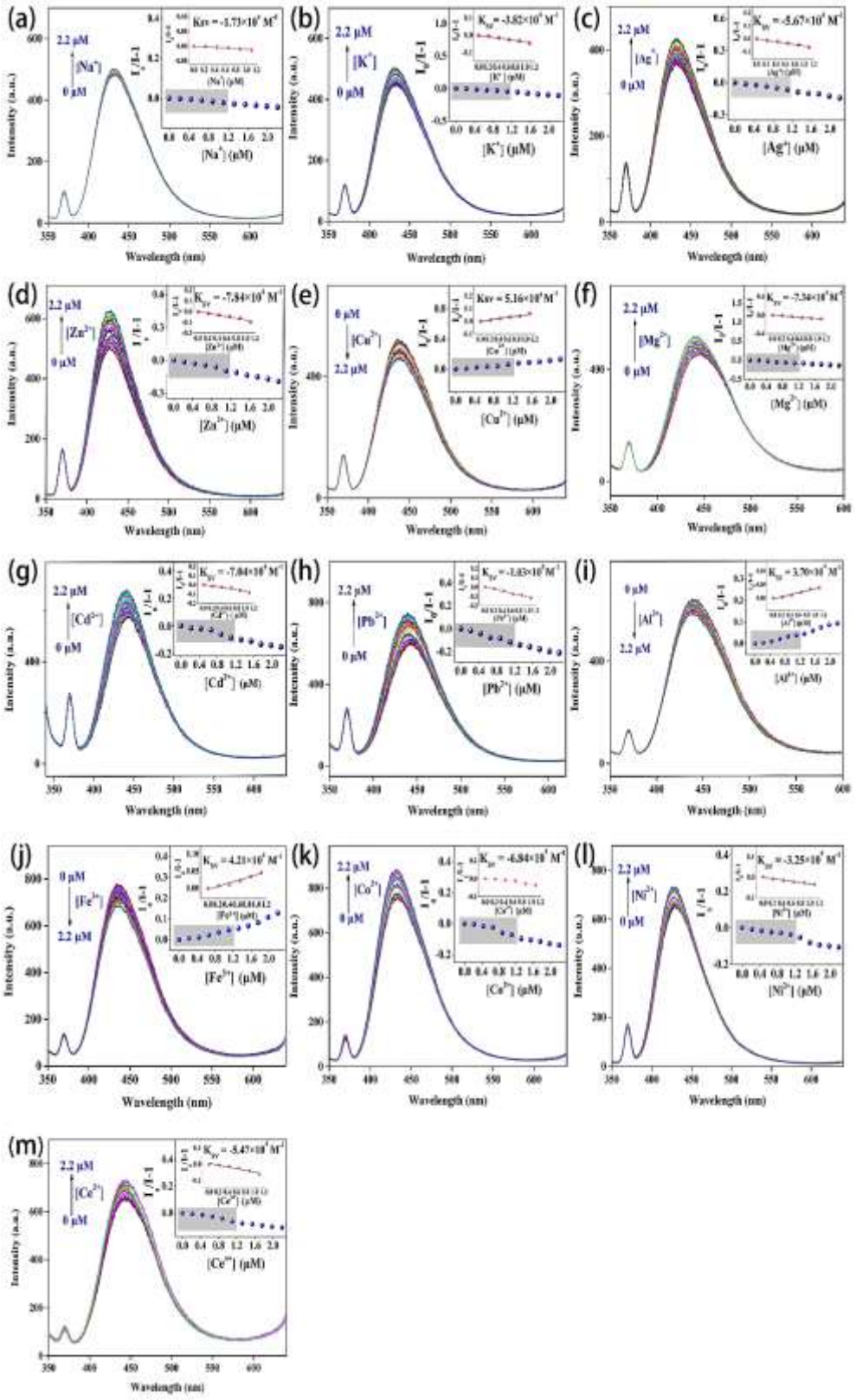

Figure S2. Fluorescence response of UiO-66-NH_2 for detection a) Na^+, b) K^+, c) Ag^+, d) Zn^{2+}, e) Cu^{2+}, f) Mg^{2+}, g) Cd^{2+}, h) Pb^{2+}, i) Al^{3+}, j) Fe^{3+}, k) Co^{2+}, l) Ni^{2+} and m) Ce^{3+} with different concentrations. Inset graphs show the corresponding fitting lines at low concentrations.

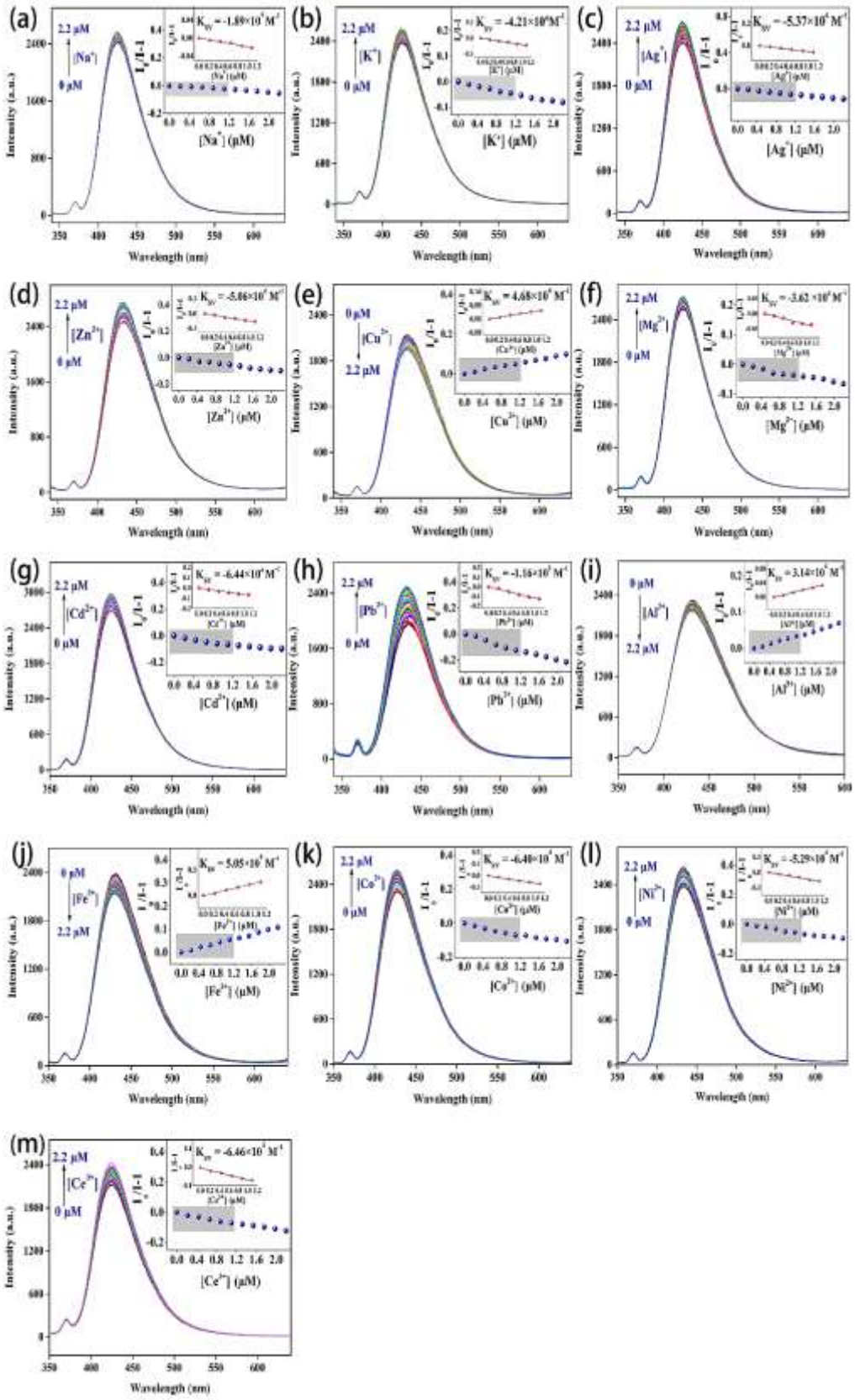

Figure S3. Fluorescence response of LTP@UiO-66-NH_2 for detection a) Na^+, b) K^+, c) Ag^+, d) Zn^{2+}, e) Cu^{2+}, f) Mg^{2+}, g) Cd^{2+}, h) Pb^{2+}, i) Al^{3+}, j) Fe^{3+}, k) Co^{2+}, l) Ni^{2+} and m) Ce^{3+} with different concentrations. Inset graphs show the corresponding fitting lines at low concentrations.

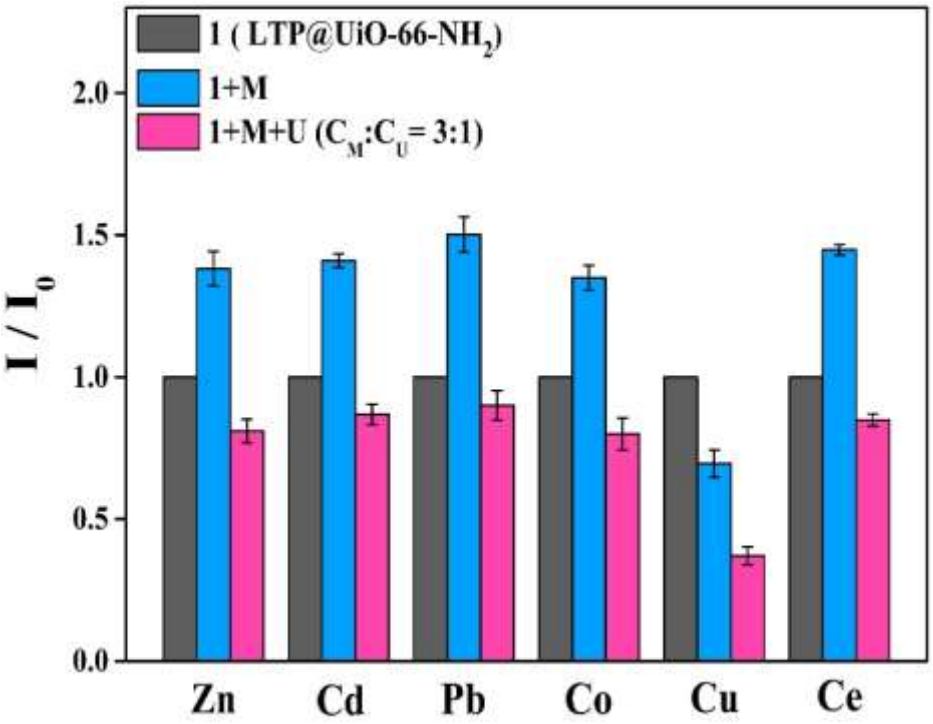

Figure S4. Fluorescence response of U(VI) under different interfering ions for LTP@UiO-66-NH_2 [$C_{[M]}$:$C_{U(VI)}$ =3:1 with $C_{U(VI)}$ of 2.5 μM].

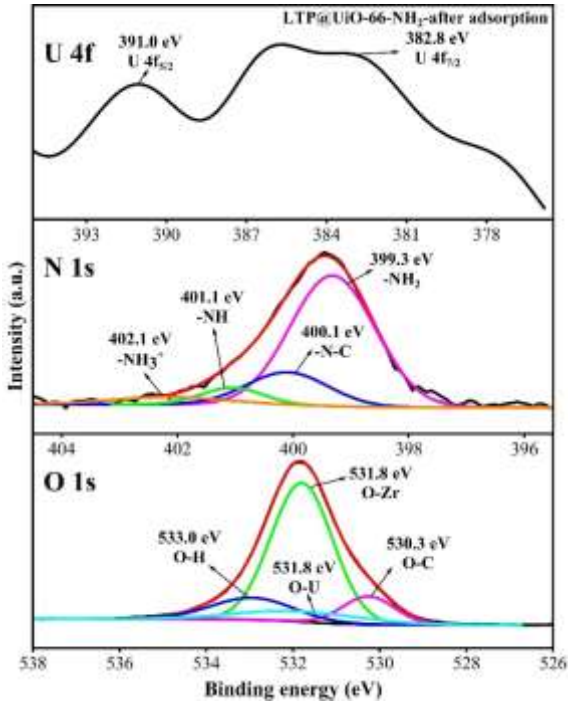

Figure S5. XPS spectra (U4f, N1s and O1s) of LTP@UiO-66-NH_2 after U(VI) adsorption.

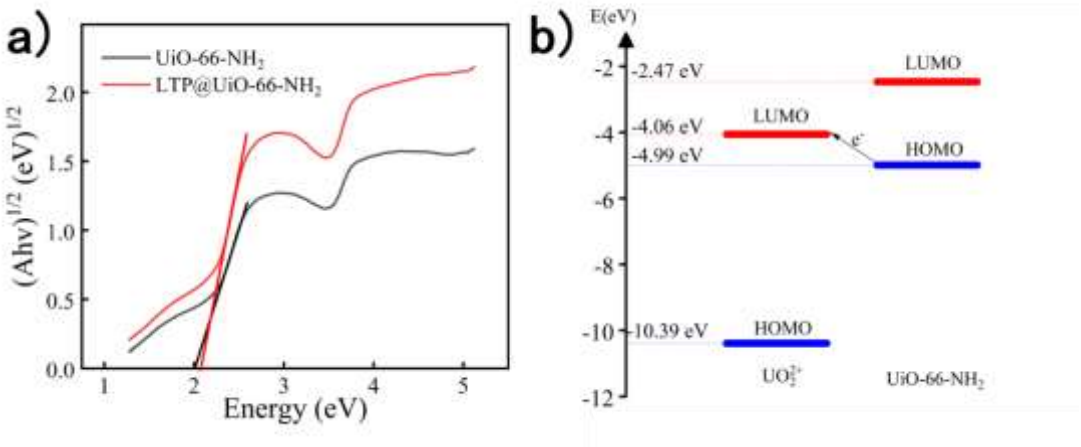

Figure S6. (a) Band gaps of UiO-66-NH_2 and LTP@UiO-66-NH_2, (b) energy levels of UiO-66-NH_2 and UO_2^{2+}.

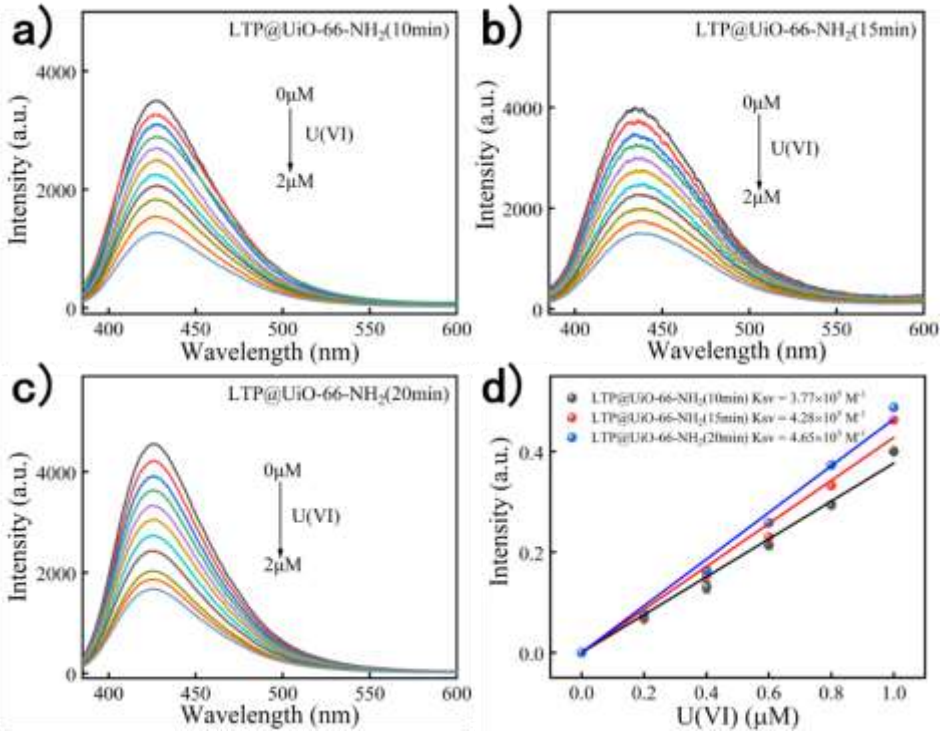

Figure S7. (a-c) Fluorescence response toward U(VI) using LTP@UiO-66-NH_2 with different plasma treatment time for (a) 10 min, (b) 15 min and (c) 20 min, (d) the corresponding Ksv values.

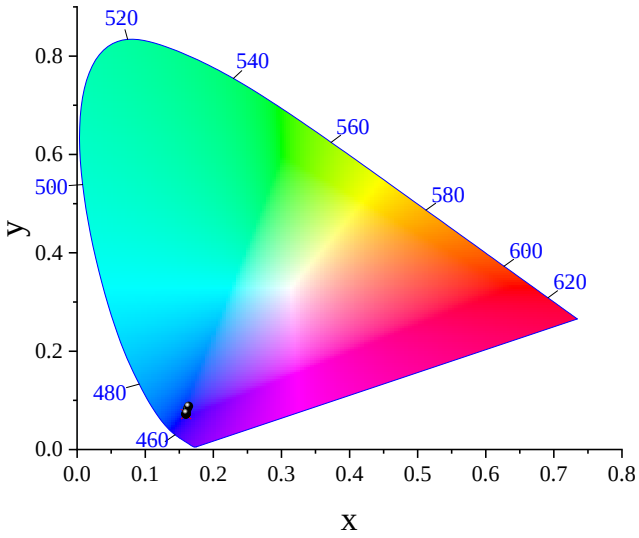

Figure S8. CIE chromaticity diagram of LTP@UiO-66-NH_2 after recognition of U (VI).

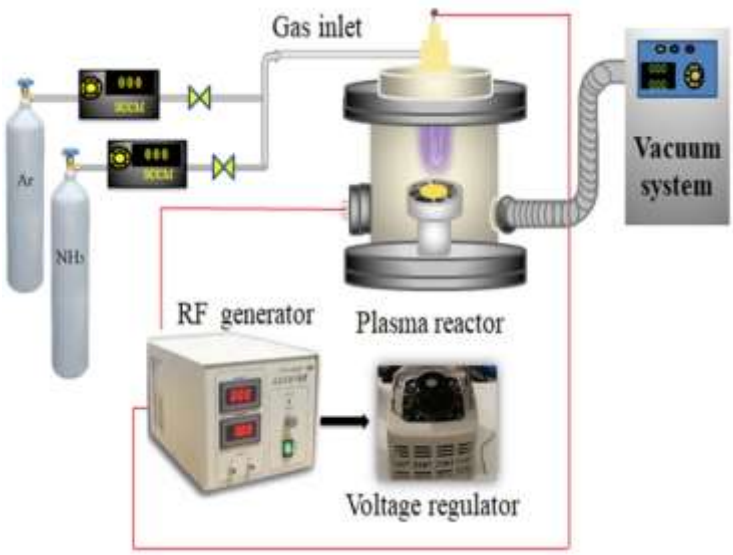

Scheme S1. Illustration of low-temperature plasma reaction equipment.

Table S1. Inter-day and intra-day precision and accuracy assay for determination of U(VI) using LTP@UiO-66-NH_2 as fluorescence probe.

Added (μM)	Measured (μM) (mean±SD, n=5)	RSD (%)	Recovery (%)
Intra-day			
0.4	0.41±0.010	2.44	102.5
1.6	1.57±0.031	1.97	98.1
16.0	16.43±0.36	2.19	102.7
Inter-day			
0.4	0.39±0.012	3.08	97.5
1.6	1.66±0.030	1.81	103.8
16.0	16.73±0.17	1.02	104.6

Table S2. Determination of U(VI) in real samples using LTP@UiO-66-NH_2 as fluorescence probe.

Sample	Added (μM)	Measured (μM) (mean±SD)	RSD (%)	Recovery(%)
Yihai Lake	0.2	0.19±0.07	3.68	95.0
	4.0	4.15±0.12	2.89	103.8
	12.0	12.73±0.23	1.81	106.1
Tap Water	0.2	0.21±0.0080	0.38	105.0
	4.0	3.89±0.12	3.08	97.3
	12.0	12.52±0.23	1.84	104.3

Table S3. A comparison of Ksv and LOD of MOF-based fluorescence probes towards U(VI) detection in water at room temperature (298K).

MOF	K_{SV} / [M^{-1}]	LOD	Ref
Co(II)-MOF, $[Co_2(\text{-dmimpym})(nda)_2]_n$	1.1×10^4	13.2 μM	S1
$[Eu\ (TIBTC)(DMF)_3]_n$ (CP-1)	4.0×10^3	11.0 μM	S2
$[Zn(HL)(bipy)_{0.5}(H_2O)]\cdot 2H_2O$	4.0×10^4	0.40 μM	S3
$[Eu_2(TATAB)_2]\cdot 4H_2O\cdot 6DMF$	8.4×10^4	0.90 μM	S4
$[Cd_3(L)_2(bipy)\ (H_2O)_2]\cdot H_2O$	2.67×10^4	-	S5
$[Tb(BPDC)_2]\cdot(CH_3)_2NH_2$ (DUT-101)	1.03×10^4	0.04 μM	S6
$[Eu_2(MTBC)(OH)_2(DMF)_3(H_2O)_4]\cdot 2DMF\cdot 7H_2O$	3.6×10^3	1.30 μM	S7
LnCP 1, $[Ln(ox)(L)]_n$ (ox = oxalate, HL = N,N'-dipropionic acid imidazolium, Ln = Eu)	6.19×10^4	1.95 μM	S8
$UiO\text{-}66\text{-}NH_2$	9.94×10^4	0.20μM （47.61 ppb）	This work
$LTP@UiO\text{-}66\text{-}NH_2$	1.81×10^5	0.08 μM （19.04 ppb）	This work

Table S4. N content of UiO-66-NH_2 and corresponding LTP@UiO-66-NH_2 under different plasma treatment time.

Sample	Plasma treatment time (min)	N content (Weight %)
UiO-66-NH_2	0	3.59
LTP@UiO-66-NH_2 (5min)	5	4.17
LTP@UiO-66-NH_2 (10min)	10	4.30
LTP@UiO-66-NH_2 (15min)	15	4.48
LTP@UiO-66-NH_2 (20min)	20	4.52

References:

[S1] Chen, W.-M.; Meng, X.-L.; Zhuang, G.-L.; Wang, Z.; Kurmoo, M.; Zhao, Q.-Q.; Wang, X.-P.; Tung, B. C.-H.; Sun, D. *J. Mater. Chem. A* **2017**, *5*, 13079-13085.

[S2] Wang, Y.; Xing, S. H.; Zhang, X.; Liu, C. H.; Li, B.; Bai, F. Y.; Xing, Y. H.; Sun, L. X. *Appl. Organomet. Chem.* **2019**, *33*, e4898.

[S3] Hou, J.-X.; Gao, J.-P.; Liu, J.; Jing, X.; Li, L.-J.; Du, J.-L. *Dyes Pigments* **2019**, *160*, 159-164.

[S4] Li, L.; Shen, S.; Su, J.; Ai, W.; Bai, Y.; Liu, H. *Anal. Bioanal. Chem.* **2019**, *411*, 4213-4220.

[S5] Liu, J.; Hou, J.-X.; Gao, J.-P.; Liu, J.-M.; Jing, X.; Li, L.-J.; Du, J.-L. *Mater. Lett.* **2019**, *241*, 184-186.

[S6] Ye, J.; Bogale, R. F.; Shi, Y.; Chen, Y.; Liu, X.; Zhang, S.; Yang, Y.; Zhao, J.; Ning, G. *Chemistry* **2017,** *23* , 7657-7662.

[S7] Liu, W.; Wang, Y.; Song, L.; Silver, M. A.; Xie, J.; Zhang, L.; Chen, L.; Diwu, J.; Chai, Z.; Wang, S. *Talanta* **2019**, 196, 515-522.

[S8] Cai, B.; Meng, Y.-N.; Zhu, M.-E.; Yang, Y. *J. Chem. Res.* **2020**, *45*, 130-135.